nzsee
NEW ZEALAND SOCIETY FOR EARTHQUAKE ENGINEERING

Unbonded post-tensioning of face loaded URM cavity walls under semi-cyclic and dynamic loading

U.J. Maduh & D. Dizhur
University of Auckland, Auckland.

H. Tocher
Holmes Consulting, Auckland.

N. Slavin
California Polytechnic State University, San Luis Obispo, United States.

ABSTRACT

An unbonded post-tensioning (PT) system installed into full-scale face loaded (out-of-plane) URM cavity walls using threaded rod and steel anchor plates spanning the cavity was investigated through experimental testing. Two different cavity wall typologies were tested: (1) two single clay brick leaves separated by an air cavity and (2) a two-leaf solid clay brick wall with an external single leaf brick layer separated by an air cavity. The PT walls were tested under semi-cyclic and dynamic shake-table loading. The tested PT system suppressed mid-span wall displacements, resulting in wall responses that were constrained well below geometric instability. Load-carrying capacity increased markedly up to 1500% when compared to cavity walls without post-tensioning. PT loads were varied to determine whether rod tension could be activated by vertical wall arching displacement. Upon preliminary analysis of the unbonded PT system, it was concluded that post-tensioning provides a cost-effective and constructible solution to considerably improve the performance of URM cavity walls.

1 INTRODUCTION

Unreinforced masonry (URM) buildings constructed using clay brick cavity walls are widely prevalent in European countries, North America, Australia, and New Zealand. Cavity walls are historically used because they are comparatively lighter-weight, have excellent thermal insulation properties, and provide protection from external moisture ingress (Giaretton et al., 2016a; Giaretton et al., 2016b; Graziotti et al., 2016). The 1931 Hawk's Bay earthquake in New Zealand (Brodie & Harris, 1933), the 1989 Newcastle earthquake in Australia (Griffith, 1991; Page, 1996), the 1994 Northridge earthquake in the USA (Klingner, 1994), the

2009 L'Aquila earthquake in Italy (Vicente et al., 2012), and the 2010/2011 Canterbury earthquakes in New Zealand (Dizhur et al., 2013) have highlighted the poor performance of URM cavity wall buildings. Post-earthquake assessments have shown that structural damage and collapse of URM buildings were mostly due to out-of-plane failure mechanisms (Graziotti et al., 2016). The vulnerability of cavity wall buildings to out-of-plane overturning mechanisms is associated with the walls being slender and lightly loaded (Graziotti et al., 2016). Poor boundary restraints and lack of connection to horizontal structural diaphragm elements as well as insufficient connections between the exterior and interior leaves of a cavity (Giaretton et al., 2016b; Graziotti et al., 2016) further contribute to vulnerability of cavity wall buildings.

Limited experimental research has been conducted on performance improvement of URM cavity wall buildings against lateral seismic loading. Walsh et al. (2015) performed airbag tests using a variety of cavity ties installed at different spacings to investigate the out-of-plane (OOP) response of retrofitted cavity walls in one-way vertical flexure. The aim was to enable semi-composite to composite behaviour of URM cavity wall leaves when subjected to induced seismic OOP loading. Giaretton et al. (2016b) presented the results of shaking table testing performed on five cavity walls. The study weighed on evaluating the use of additional ties and timber strong-backs as functional seismic retrofit solutions. Graziotti et al. (2016) reported the results of shaking table testing performed on URM single leaf walls and cavity walls, with the focus to understand the seismic behaviour of the walls, their failure mechanisms, and the effects of boundary conditions and degree of connection between the two leaves. Derakhshan et al. (2018) performed quasi-static airbag tests to investigate seismic retrofit of out-of-plane loaded cavity walls with improved cavity connections, in the form of either standard bent metal ties or proprietary helical anchors, to maintain the cavity gap until a wall failure mechanism formed.

Although some limited research has been conducted on the improvement of URM cavity walls seismic performance, there is still limited literature on experimental validation, particularly dynamic tests, to support suitable seismic retrofit of cavity walls. Described herein are the out-of-plane shaking table tests on post-tensioned URM cavity walls. Two different cavity wall typologies were tested: (1) two single clay brick leaves separated by an air cavity and (2) two-leaf solid clay brick walls with an external single leaf brick layer separated by an air cavity. Post-tension loads were varied to determine whether rod tension could be activated by vertical wall arching displacement. The test set-up was constructed to induce OOP one-way bending behaviour in the specimens and to allow a general overview of dynamic performance in retrofitted conditions.

2 EXPERIMENTAL STUDY

2.1 Test wall specifications

Five purpose-built full-scale URM wall specimens shown in Figure 1 were used for the experimental testing programme reported herein. The walls were one-way vertically spanning 3000 mm high and 1150 mm wide. The wall height was chosen to replicate a typical upper storey in a URM building. Two of the walls tested with a PT system were single-single cavity walls, denoted as "1+1", with a thickness of 275 mm and massed approximately 1430 kg. The other three walls were double-single cavity walls, denoted as "2+1", with a thickness of 395 mm and massed approximately 2150 kg. An approximately 55 mm wide air cavity separated the wall specimens. These selected wall configurations are often found in New Zealand URM buildings, with the double-single cavity walls commonly but not exclusively found on lower floors. The cavity width in all the walls was specified as 55 mm, or approximately half the thickness of a standard brick.

Figure 1: Wall specimens

2.2 Test wall construction

The double leaf walls were constructed using a common bond pattern, with one header course after every three stretcher courses, by an experienced bricklayer under supervision. Vintage clay bricks recycled from a 1930s URM building were used for the walls' construction. The dimensions of the masonry units were 230 x 110 x 75 mm. Mortar joints were nominally 15 mm thick with 1:2:9 cement:lime:sand composition by volume as used by Giaretton et al. (2016b). The material testing in compliance with ASTM (2013, 2014a, 2014b) was undertaken on three brick high masonry prisms and mortar cubes to determine the average material properties. The mean compressive strengths of bricks and mortar cubes, in axial compression, were 22.7 MPa (14 samples, CoV 45%) and 2.0 MPa (16 samples, CoV 45%). The brick strength is between the benchmark value for the categories Soft and Medium, whereas the mortar strength corresponds to the upper end of the category Soft, as defined in Tables C8.3 and C8.4 of the New Zealand Guidelines (MBIE, 2017) for the Seismic Assessment of Existing Buildings (Tocher et al., 2019). The average compressive strength of the masonry prisms was 11.5 MPa (10 samples, CoV 19%) and corresponds to a mid-range masonry compressive strength as defined in Table C8.5 of the Guidelines (Tocher et al., 2019).

2.3 Retrofit techniques

The URM cavity wall specimens in the as-built condition contain wire ties of 4.0 mm steel bent into hoops to connect the leaves across the cavities. The wire hoops were notched to simulate corrosion and inserted every six courses, alternating between a pair of hoops and a single hoop to create an offset pattern (Tocher et al., 2019). This tie placement was a common practice in the construction of typical URM buildings (Derakhshan et al., 2018). In addition to vertical PT rods, the retrofitted wall specimens contained 6 mm diameter screws with a length of approximately 240 mm that spanned the cavity to connect the two leaves, spaced at approximately 460 mm on centre horizontally and 400 mm on centre vertically. These cavity ties were used to prevent buckling of the walls under high PT forces. The post-tensioning bar was a 16 mm diameter high tensile threaded 8.8 grade steel rod. At the base, three separate methods were tested to anchor the PT rod to the wall. For 1+1 walls, the rod was positioned at the centre of the cavity wall and inserted into a 20 mm diameter hole at the centre of a 25 mm thick horizontal steel plate. A brick was removed from the third course of each leaf, allowing the plate to bear directly on the fourth course (Fig. 2a). For 2+1 walls, a more constructible method involved drilling through the double leaf face and inserting two short threaded 8.8 grade steel rods for a similar plate to bear on. An alternate system developed for 2+1 walls involved pouring grout into the cavity up to the fifth course of bricks with the PT rod embedded in the grout (Fig. 2b). The method was applied to identify which would improve the performance of the wall. With this anchorage method, small plates were placed at the end of the rod, and four additional cavity ties were set through the

grout to prevent pull out of the PT rod or the grout plug. At the top of the wall, the threaded steel rod was bolted through a 450 x 450 x 8 mm steel top plate, where a large washer was placed onto a load cell to distribute the load evenly (Fig. 2c). A hydraulic jack placed at the top of the wall pre-tensioned the threaded steel rod to different forces depending on the test, thereby inducing compression in the wall.

(a) Wall 1+1 bottom anchor using a steel plate

(b) Wall 2+1 bottom anchor using grouting

(c) Top elements and a steel plate

Figure 2: Post-tensioned anchor connections

3 TESTING PROGRAMMES

3.1 Semi-cyclic testing

The first stage of testing was performed on cavity wall specimens using a system of airbags to apply a uniformly distributed semi-cyclic loading, imitating a lateral seismic load generated in the out-of-plane direction (Fig. 3). One 1+1 wall and two 2+1 walls were tested with PT retrofits using the static airbag method. The level of pre-compression applied to the wall represents the typical stress levels attributed to both overburden compression due to upper storeys and compression due to post-tensioning (Ismail et al., 2012). Timber members bolted to a strong concrete floor and bearing directly on the first course of bricks restrained each wall at its base. A timber stringer was connected at course 31 using a mechanical screw system consisting of three double threaded 8mm diameter and 240 mm long screws (Python MT) and timber joists connected the stringer to a strong concrete wall. A loose bolted connection was installed between the joists and the strong wall to allow free rotation of the top of the wall and prevent horizontal translation. To allow each wall to be considered pinned at top and base, the upper and lower connections were designed to recreate in-service conditions of URM walls in a post-retrofitted state (Tocher et al., 2019).

The airbags reacted against the timber reaction frame (Fig.3a) to the right of the URM wall specimen. The airbags were sandwiched between the timber and a layer of polystyrene (Fig. 3b) to ensure a better distribution of applied pressure (Tocher et al., 2019). In addition to four load cells measuring out-of-plane force, a fifth load cell was placed between the PT rod anchorage and the top of the wall to measure the PT force exerted on the wall specimens when airbags were inflated. A displacement-controlled loading was applied by inflating and deflating the airbags, and multiple cycles were applied to the wall specimens.

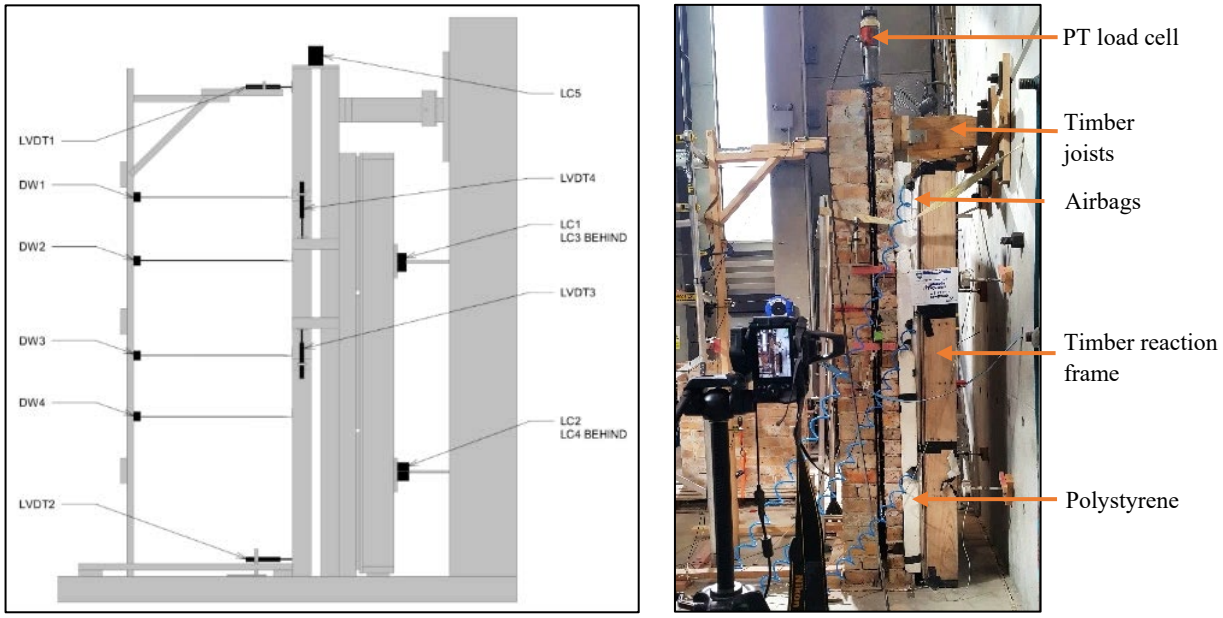

(a) Instrumentation layout

(b) Wall test set-up showing 2+1 arrangement

Figure 3: Instrumentation layout and test set-up for semi-cyclic testing

3.2 Dynamic (shake table) testing

Testing of one 1+1 PT wall and one 2+1 PT wall was performed using a shake-table with the test set-up shown in Figure 4. The protection and restraint frame was designed and built onto the shake-table platform to provide wall-top restraint and to protect the testing instrumentation. Two stiff steel angles, together with timber members bolted and bearing directly on the first course of bricks were used to restrain the wall at the base and ensure that lateral movement of the wall base was prevented. A timber stringer was connected at course 31 using a mechanical screw system consisting of three double threaded 8mm diameter and 240 mm long screws (Python MT) in tern connected to four timber joists (representing a timber diaphragm) connected the stringer to the steel frame fixed directly onto the shake table. The frame was braced using steel bars and steel braces to withstand the load transfer from the wall into the frame. A pined (bolted) connection was installed between the timber diaphragm and the steel frame to allow free rotation of the top of the wall and prevent horizontal translation. Six accelerometers were installed at the bottom, middle, and top of the walls and on the shaking table in order to record the effective horizontal acceleration produced, and seven string potentiometers were attached at the bottom, middle and top of the wall and on the shaking table to measure the differential displacements of the walls.

Two ground motion records from February 2011 M6.3 Christchurch earthquake (Christchurch Botanical Garden, CBGS_S01W, chosen for its repeated high-displacement reversals and Lyttleton Port Company, LPCC_S80W, chosen for its rapid and violent shaking) were reproduced using shake-table and applied perpendicular to the longitudinal direction of the tested walls. The acceleration amplitude of the reproduced earthquake records was incrementally increased from 10% to 125% until the maximum displacement of the shake table (±180 mm) was reached.

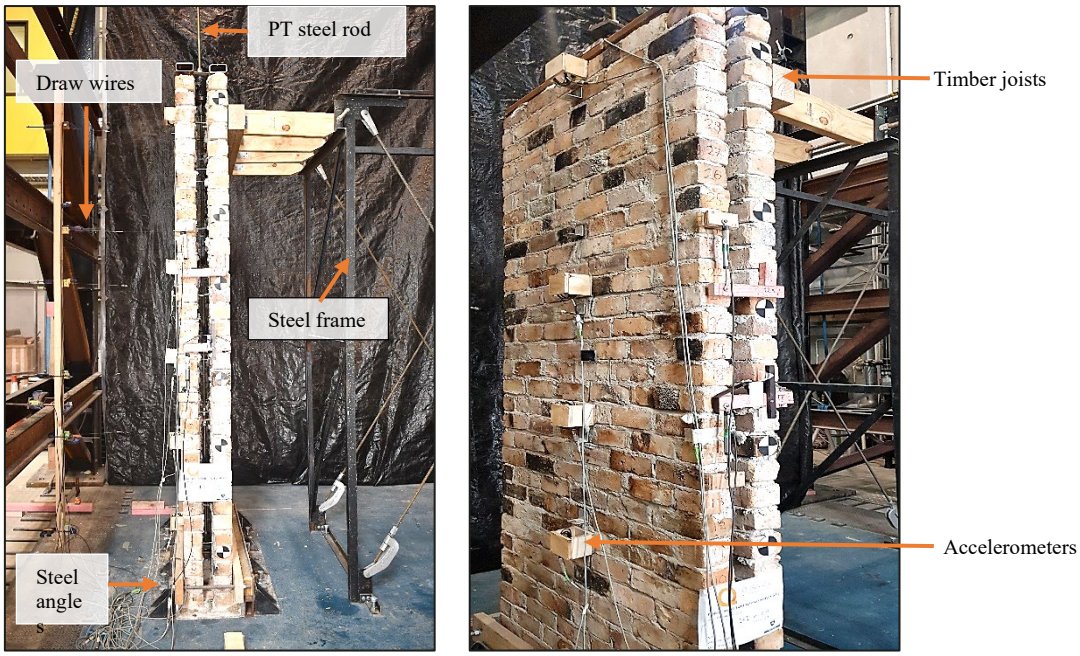

(a) Front view (b) Side view

Figure 4: Test wall set-up of shaking table test showing 1+1 arrangement

4 RESULTS AND DISCUSSION

4.1 Semi-cyclic testing results

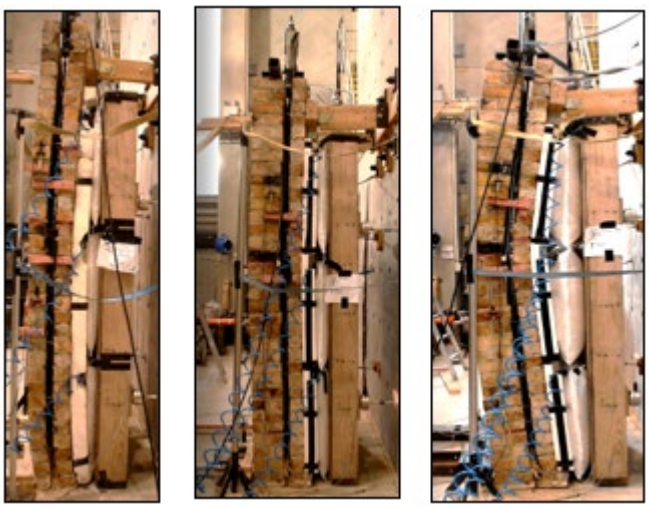

(a) Wall 1+1 (b) Wall 2+1 (c) High loading

Figure 5: Loading of test walls

Figure 5 shows the semi-cyclic testing of PT wall specimens. The first wall tested using the static airbag method was a single-single (1+1) wall with an applied PT load of 80 kN. The wall reached a maximum total out-of-plane force of 16.4 kN during testing, which was approximately 15 times greater than the 1.1 kN as-built capacity of the wall (Fig. 6a). At ultimate loading, the PT 1+1 wall failed in shear between courses 3 and 4 in both leaves (Fig. 6b). The crack location corresponds to the boundary between the PT wall and the non-PT part of the wall below the bottom rod anchorage point. The post-tensioned part of the wall acted closely resembling a rigid object, rotating about the top restraint and deformed at the bottom three courses, where the wall was not post-tensioned.

After completing the 80kN PT test, wall 1+1 was realigned to its original position and subjected to additional testing. Tests were conducted at initial PT loads of 10 kN and 34 kN to determine if a similar lateral force capacity could be reached with lower PT loads. Total out-of-plane loads reached a maximum of approximately 10 kN for the two tests being referenced. A mid-height displacement of 15 mm at draw wire 2 (see Fig. 3) was required to reach the 10 kN lateral force for the 34 kN PT test, while a displacement of 30 mm at draw wire 2 (DW2) was required to reach the same capacity for the 10 kN PT test (Fig. 6c). Displacements were limited for both 10 kN and 34 kN PT loads because the back leaf of the wall becoming in contact with the PT rod. While monitoring the top load cell, it was noticed that PT load slowly dropped (as

the wall displaced) during the 80 kN PT test due to oil leakage but remained at approximately 90% of the original load following testing. As the DW2 displacement reading increased, the wall had a tendency to arch in turn increasing the PT loading to 23 kN (130% increase) for the 10 kN PT test (Fig. 6d). The tested wall with 80kN PT loading, exhibited minor out-of-plane rotation as the PT load was applied using the hydraulic jack; hence the negative displacement of DW2 is shown in Figure 6d.

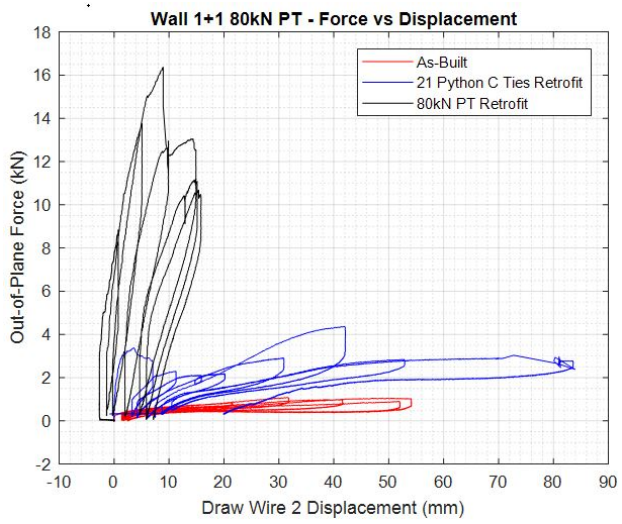

(a) 80 kN PT: out-of-plane force vs displacement

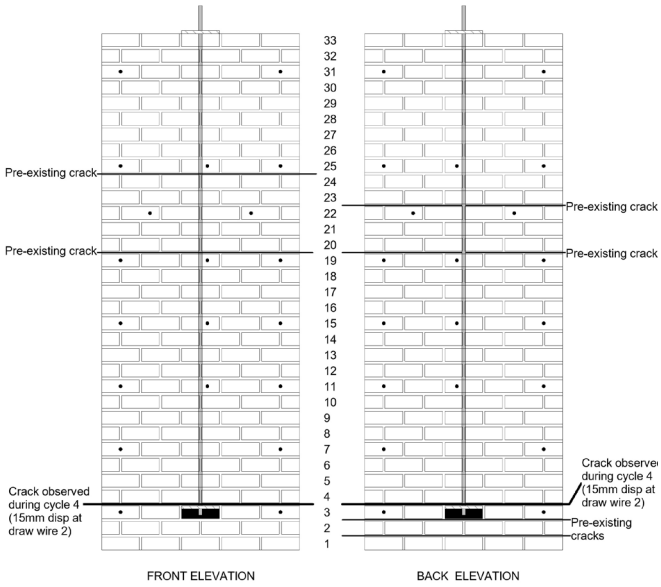

(b) Cracking patterns during 80 kN PT test

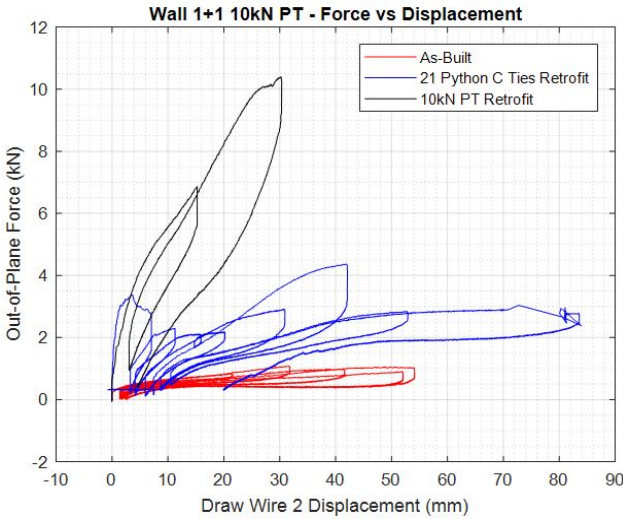

(c) 10 kN PT: out-of-plane force vs displacement

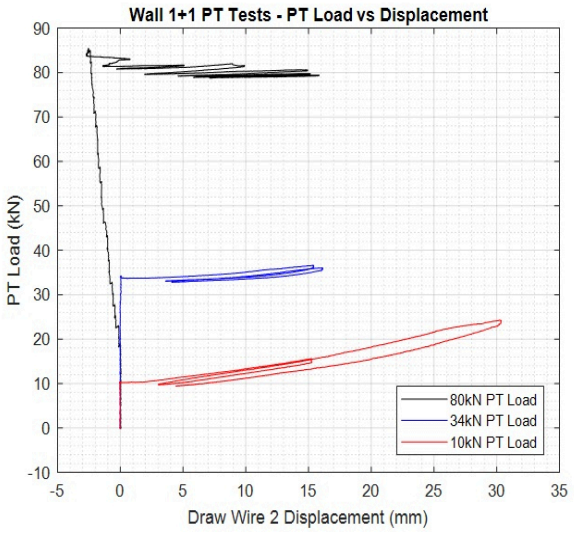

(d) PT load vs displacement

Figure 6: Wall 1+1 Semi-Cyclic Testing

Two 2+1 walls were tested semi-cyclically with a PT retrofit system. The first wall 2+1 was tested with 50 kN PT load and with the lateral pressure being applied onto the single leaf. The total out-of-plane force reached 13 kN, which was approximately three times greater than the as-built capacity of the wall (Fig. 7a). Details of the walls tested in retrofitted condition using semi-rigid ties can be found in Tocher et al. (2019).

The double-single (2+1) wall uniformly deflected together with the PT rod as the airbag pressure was applied. After observing the force vs displacement plot shown in Figure 7a, it was hypothesised that the force

capacity may not have reached an inelastic limit but would increase at higher displacements, prompting extended testing of the subsequent wall 2+1.

The second 2+1 wall specimen was subjected to 80 kN PT load and initially tested with the airbag pressure applied onto the double leaf face. The wall reached an out-of-plane force of 26 kN before shear failure of the masonry occurred at the top of the wall. The 26 kN capacity was approximately 400% greater than the capacity of the wall in its as-built condition. The second 2+1 wall was rotated and tested again, this time with the single leaf being loaded. The wall started with a PT load of 80 kN and was pushed through various cycles, which resulted in a drop of the out-of-plane capacity of the retrofit system (Fig. 7b). The peak out-of-plane force reached during testing was 39.1 kN at 110 mm displacement, corresponding to approximately 2.0g of acceleration and 500% greater than the as-built test of the wall in the same orientation. PT load was increasing throughout testing due to wall arching action reaching almost 110 kN (140% of the original PT load) (Fig. 7c), which could be attributed to cracking of the grout anchorage at the base of the PT rod of wall

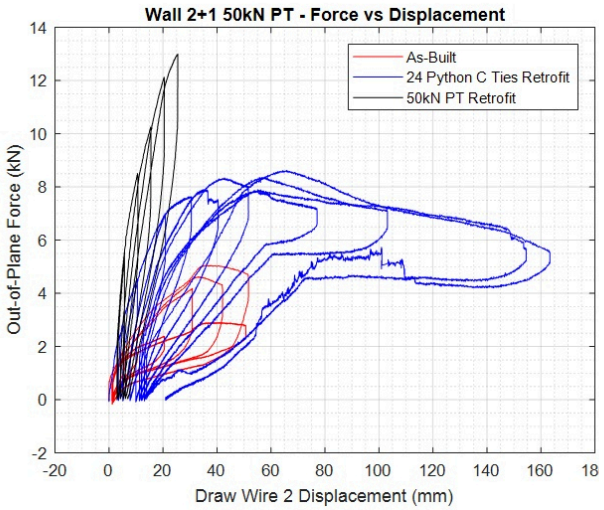

(a) 50 kN PT: out-of-plane force vs displacement

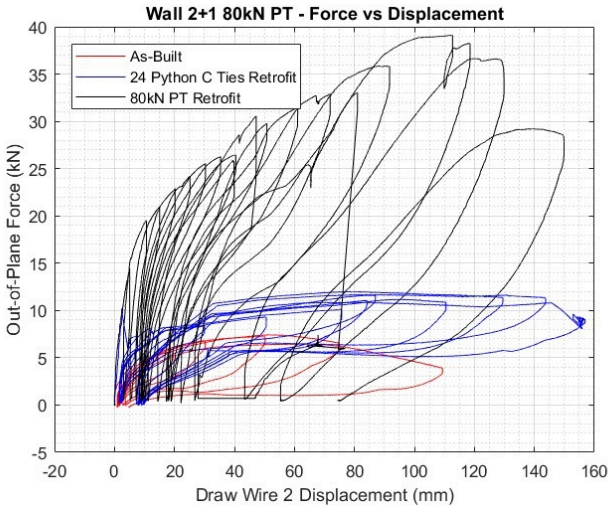

(b) 80 kN PT: out-of-plane force vs displacement

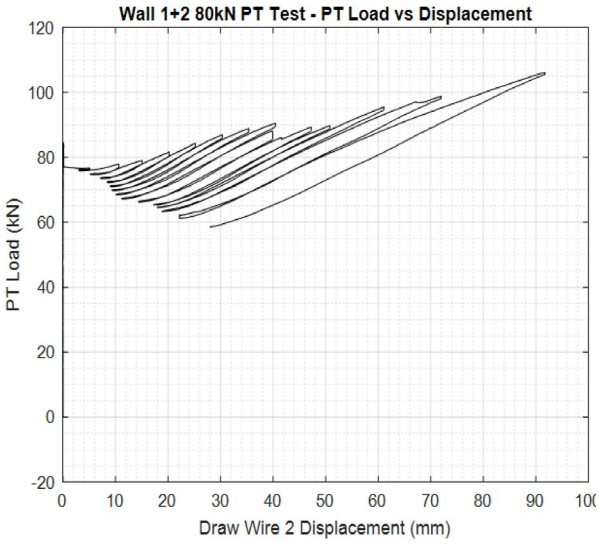

(c) 80 kN PT: PT load vs displacement, wall loaded on the single leaf

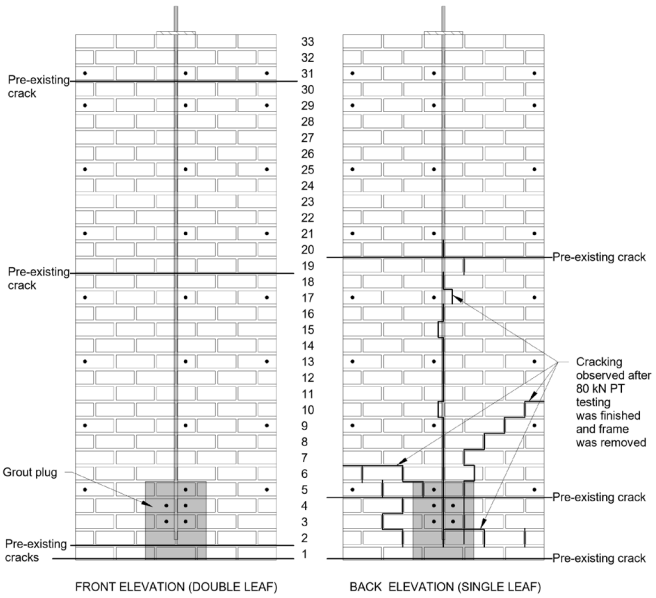

(d) Cracking patterns during after 80 kN PT test

Figure 7: Wall 2+1 Semi-Cyclic Testing

1+2. After finishing testing and removing the timber reaction frame, extensive cracking was noticed on the single leaf near the grout plug and continuing up along the PT rod (Fig. 7d).

4.2 Dynamic testing results

At the end of each stage of the shaking table testing sequence, a detailed survey was carried out to check possible evidence of damage having affected the walls. The results in terms of damage pattern and failure modes (Fig. 8), wall height against peak acceleration normalised with peak ground acceleration (PGA), and displacements measured at input ground motions are presented.

At the time of writing the test results from CBGS records are being processed and hence only results from LPCC are being discussed herein. The post-tensioned walls were first subjected to the ground motion of the Lyttleton earth (LPCC) earthquake, with 125% of LPCC being the maximum acceleration the shake table was able to generate. The post-tensioned load applied to the walls was 80 kN. The use of post-tensioning increased the compression loading significantly against the formation of cracks even at high acceleration intensities. The single-single (1+1) cavity wall exhibited a rigid body behaviour and did not experience any noticeable damage after tested under, 7 earthquake records corresponding to LPCC-125% at a PGA = 1.03g. The post-tensioned load was reduced to 22 kN, and testing was repeated. Cracking was initiated between coarse 19 and 20 on the inner leaf of 1+1 wall after testing at 125% of LPCC with the maximum recorded PGA of 1.21g.

The double-single (2+1) cavity wall subjected to a post-tensioned load of 22 kN did not experience any form of cracks or noticeable damage with increasing shaking intensity until after testing under a cycle at LPCC-125% (PGA = 1.1g), where cracking was initiated at coarse 17 on the solid leaf.

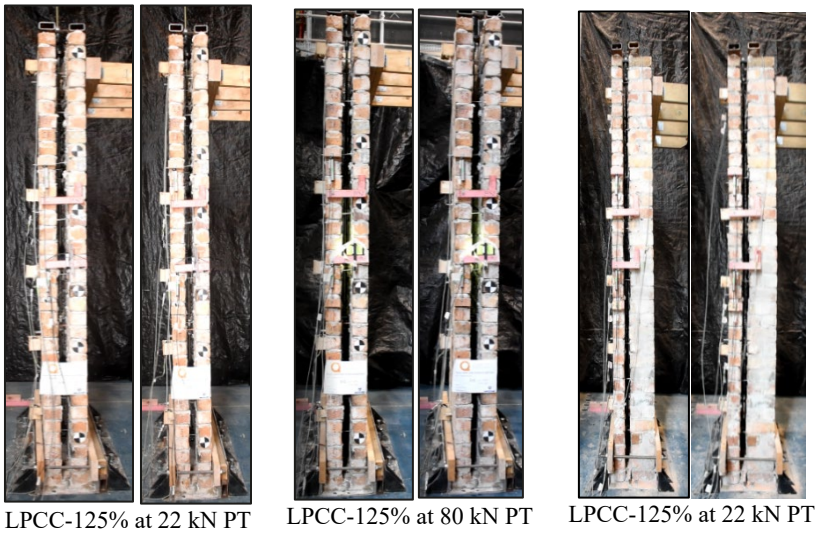

Figure 8: Failure modes of single-single and double-single cavity wall

The acceleration profile at 125% of LPPC ground motion presented in Figure 9a was used to compare the peak acceleration of each wall. The mid-height acceleration at 22 kN PT load for wall 1+1 was approximately 122% of the PGA whereas wall 2+1 recorded 137% of the PGA, an increase of 15%. At the top of the wall, the recorded acceleration difference between the two walls was 52% of the PGA. The response of post-tensioned variation for Wall 1+1 is shown in Figure 9b. The top acceleration recorded when 22 kN PT load was applied to the wall was approximately 156% of PGA. The value increases to 280% at 80 kN PT load. Increase in post-tensioned load resulted in higher acceleration at the top of the wall, similar to observations by Giaretton et al. (2016a), where the use of strong backs produced an increase in acceleration.

Figure 10a presents the lateral displacement for the wall specimens versus height at 125% of LPCC at 22 kN PT load. The behaviour of the walls was similar to that of a vertically oriented simply supported beam fixed at the base (Giaretton et al., 2016b). For 1+1 wall, the maximum drift at mid-height was 1.75% whereas it was 1.07% for wall 2+1. At the top of the wall, the drift reduced to 0.4% for wall 1+1 and 0.57% for wall 2+1. Wall 1+1 showed a similar behaviour pattern when compared to a post-tensioned variation (Fig. 10b) with about 38% decrease in displacement from 22 kN to 80 kN PT load, indicating improvement against the lateral seismic load of the wall. The maximum drifts observed for the 80 kN PT load were 0.58% at the top of the wall and 1.09% at mid-height. The drifts are presented in Table 1.

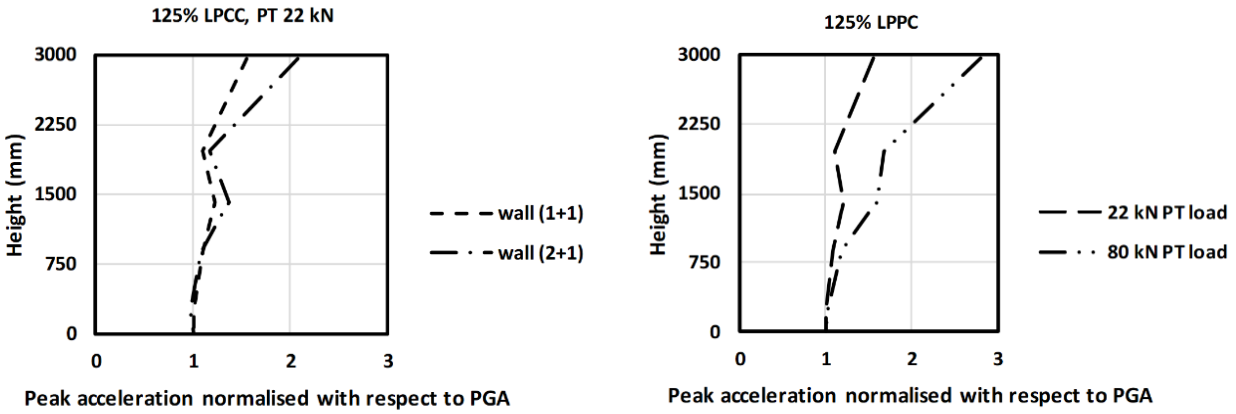

(a) 125% LPCC, PT 22 kN

(b) 125% LPCC (1+1 wall)

Figure 9: Peak acceleration versus wall-height

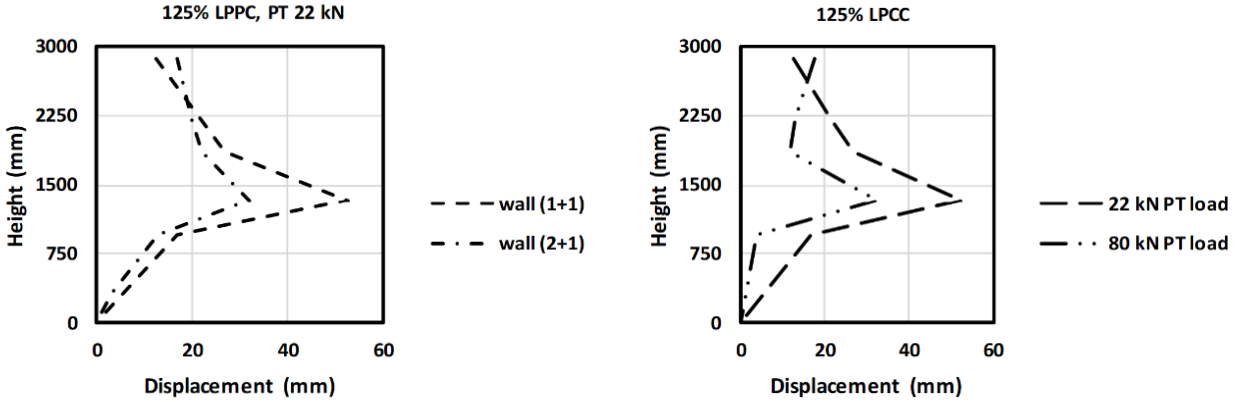

(a) 125% of LPCC, PT 22 kN

(b) 125% of LPCC (1+1 wall)

Figure 10: Horizontal displacement versus wall-height

Table 1: PGA and drifts of post tensioned walls

Ground motion	PT load (kN)	Single-single (1+1) cavity wall			Double-single (2+1) cavity wall		
		PGA	Top drift	Mid-height drift	PGA	Top drift	Mid-height drift
LPCC-125%	22	1.21g	0.4%	1.75%	1.1g	1.07%	0.57%
	80	1.03g	0.58%	1.09%	-	-	-

5 CONCLUSIONS

Semi-cyclic and shaking table experimental testing of five post-tensioned cavity walls were evaluated to investigate their retrofit capability, and the following observations were made.

Semi-cyclic testing: Post-tensioning of cavity wall specimens improved performance significantly (up to 1500%) compacted to walls in the as-built condition. The out-of-plane force capacity increased by four times (wall 1+2), six times (wall 2+1), and fifteen times (wall 1+1) when compared to as-built walls of the same configurations. The maximum total out-of-plane lateral force reached during the PT testing for a double-single wall was 39.1 kN, which is equivalent to nearly 2.0g acceleration. The post-tensioned single-single wall capacity was improved, resulting in a maximum total out-of-plane lateral force of 16.4 kN, which is equivalent to 1.2g acceleration. At ultimate lateral loading, cracking directly below where the PT rod terminated was observed, consequently leading to wall sliding. Such wall sliding is due to a limitation of the test set-up used and not a reflection of the system performance. In a real building scenario, the PT rod will extend below the floor diaphragm, which will, in turn, prevent such sliding failure modes.

Dynamic testing: The performance of the cavity walls that had the PT system significantly improved against the lateral seismic induced force. The use of post-tensioning increased the compression loading substantially against the formation of cracks at high acceleration intensities. At extreme levels of table accelerations, only minor cracks were observed on wall 1+1 and wall 2+1 (with 22 kN PT load) and no evidence of wall instability initiation when the walls experienced the maximum lateral loading that would be generated by the shake table when tested under 125% LPPC. The recorded PGA and peak acceleration at the top of the walls during the 125% LPPC earthquake were 1.21g and 1.89g for wall 1+1 with 22 kN PT load, and 1.1g and 2.29g for wall 2+1 with 22 kN PT load respectively.

Dynamic and semi-cyclic testing suggest that unbonded post-tensioning provided a cost-effective and simple method to significantly improve the seismic performance of unreinforced masonry cavity walls.

REFERENCES

ASTM. 2013. C109. Standard test method for compressive strength of hydraulic cement mortars. In. USA: American Society for Testing and Materials.

ASTM. 2014a. C67. Standard test methods for sampling and testing brick and structural clay tile. In. USA: American Society for Testing and Materials.

ASTM. 2014b. C1314. Standarsd test method for compressive strength of masonry prisms. In. USA: American Society for Testing and Materials.

Brodie, A., & Harris, B. 1933. Damage to buildings, part of Report on Hawke's Bay earthquake of 3rd February, 1931. *NZ Journal of Science, XV*, 108-114.

Derakhshan, H., Lucas, W., Visintin, P., & Griffith, M. C. 2018. Laboratory testing of strengthened cavity unreinforced masonry walls. *Journal of Structural Engineering, 144*(3), 04018005.

Dizhur, D., Moon, L., & Ingham, J. 2013. Observed performance of residential masonry veneer construction in the 2010/2011 Canterbury earthquake sequence. *Earthquake Spectra, 29*(4), 1255-1274.

Giaretton, M., Dizhur, D., Da Porto, F., & Ingham, J. M. 2016a. *Construction details and observed earthquake performance of unreinforced clay brick masonry cavity-walls.* Paper presented at the Structures.

Giaretton, M., Dizhur, D., & Ingham, J. M. 2016b. Shaking table testing of as-built and retrofitted clay brick URM cavity-walls. *Engineering Structures, 125*, 70-79.

Graziotti, F., Tomassetti, U., Penna, A., & Magenes, G. 2016. Out-of-plane shaking table tests on URM single leaf and cavity walls. *Engineering Structures, 125*, 455-470.

Griffith, M. C. (1991). *Performance of unreinforced masonry buildings during the Newcastle Earthquake, Australia.* Paper presented at the Lifeline Earthquake Engineering.

Ismail, N., Schultz, A. E., & Ingham, J. M. (2012). *Out-of-plane seismic performance of unreinforced masonry walls retrofitted using post-tensioning.* Paper presented at the Proceedings of the 15th International Brick and Block Masonry Conference, Florianópolis, Santa Caterina, Brazil.

Klingner, R. E. 1994. *Performance of masonry structures in the Northridge, California Earthquake of January 17, 1994.* Paper presented at the Restructuring: America and Beyond.

Page, A. W. 1996. Unreinforced masonry structures-an Australian overview. *Bulletin-New Zealand national society for earthquake engineering, 29*, 242-255.

Tocher, H., Slavin, N., Stanišić, A., & Dizhur, D. 2019. *URM cavity walls: Simple and experimentally proof-tested retrofit.* Paper presented at the Australian Earthquake Engineering Society, Newcastle, NSW, Australia.

Vicente, R. S., Rodrigues, H., Varum, H., Costa, A., & Da Silva, J. A. R. M. 2012. Performance of masonry enclosure walls: lessons learned from recent earthquakes. *Earthquake engineering vibration, 11*(1), 23-34.

Walsh, K. Q., Dizhur, D. Y., Shafaei, J., Derakhshan, H., & Ingham, J. M. 2015. *In situ out-of-plane testing of unreinforced masonry cavity walls in as-built and improved conditions.* Paper presented at the Structures.